



HAL
open science

Proposal of a cohesive zone model suitable for the study of bonded joints.

A. Moradi, C. Huchette, Thomas Vandellos, Dominique Leguillon

► **To cite this version:**

A. Moradi, C. Huchette, Thomas Vandellos, Dominique Leguillon. Proposal of a cohesive zone model suitable for the study of bonded joints.. 19th International Conference on Composite Materials, Jul 2013, MONTREAL, Canada. hal-01060193

HAL Id: hal-01060193

<https://onera.hal.science/hal-01060193>

Submitted on 3 Sep 2014

HAL is a multi-disciplinary open access archive for the deposit and dissemination of scientific research documents, whether they are published or not. The documents may come from teaching and research institutions in France or abroad, or from public or private research centers.

L'archive ouverte pluridisciplinaire **HAL**, est destinée au dépôt et à la diffusion de documents scientifiques de niveau recherche, publiés ou non, émanant des établissements d'enseignement et de recherche français ou étrangers, des laboratoires publics ou privés.

PROPOSAL OF A COHESIVE ZONE MODEL SUITABLE FOR THE STUDY OF BONDED JOINTS

A. Moradi^{1*}, C. Huchette¹, T. Vandellos¹, D. Leguillon²

¹ ONERA, DMSC, Châtillon, France, ² IJLRA, CNRS UMR 7190, Paris, France

* Corresponding author (azalia.moradi@onera.fr)

Keywords: *bonded joints, initiation, coupled criterion, cohesive zone model, free edge effects, adhesive thickness influence*

1 Context and objectives

Assembly design is a crucial point for structural applications. Because of a good knowledge of their failure mechanisms, bolted and riveted structures are the most widespread in industry. However stress concentrations appear around the holes in these assemblies imposing to oversize the structure. In order to avoid this phenomenon, one way consists in using an adhesive bonding. That is the reason why methods enabling to increase the confidence in bonded joints must be proposed, particularly for the initiation of a debonding.

Different classical approaches enable the study of a debonding initiation : (i) a stress or strain-based criterion [1], (ii) the coupled criterion [2] and (iii) approaches based on damage mechanics. The assessment of the advantages and the drawbacks of these different approaches in order to model the debonding initiation in 3D structures in presence of non-linear phenomena underlines the interest of using cohesive zone models (CZM) [3-4]. However, in order to use a CZM for bonded joints, suitable parameters seem to be necessary, like the adhesive thickness or the adhesive properties for instance.

That is why the first objective of this work relies essentially on the determination of the adhesive thickness influence on the initiation and on its integration into a cohesive zone model. Besides, influence studies on the shape of the law and on the mesh size have been realized in order to highlight their influence on the initiation of the bonded joint.

Then, the second objective remains in the validation of the model. For that, using the results of finite element simulations, several initiation tests with free edge effects have been studied with the coupled criterion to highlight the relevant tests enabling to

validate the stress criterion of the CZM which has been identified with tests without free edge effects.

2 Influence of the adhesive thickness on the initiation of a bonded joint

The control of the adhesive thickness during the manufacturing of the bonded assembly is difficult. Therefore it seems important to study the influence of the adhesive thickness on the initiation failure load, the initiation crack length and the displacement at initiation of a bonded joint. To investigate this question, firstly, the approach based on the use of a coupled criterion by data exploitation of elastic computations is presented. For that, a simplified 2D modeling with linear material behaviors under elastic assumptions has thus been realized.

Because it is a relevant initiation test presenting high edge effects, the Thick Adherend Shear Test (TAST) in its modified configuration [4] has been modeled. But contrary to the modeling realized in [5] the beaks on the substrates are not modeled in order to keep the edge effects. The dimensions, the boundary conditions and the load applied are illustrated on Fig. 1.

For this modeling, the substrates behavior and the adhesive behavior are considered isotropic linear elastic. The mechanical properties of the substrates and of the adhesive are respectively presented in Table 1 and in Table 2.

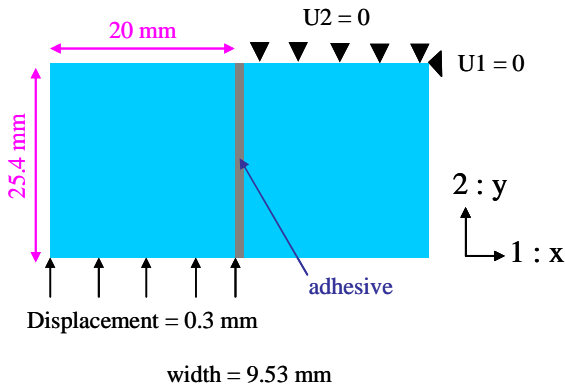


Fig. 1. Geometry, boundary conditions and load applied in the elastic computations on the modified TAST

Young Modulus (MPa)	Poisson coefficient
80000	0.3

Table 1. Mechanical properties of the substrates in Aluminum

Young Modulus (MPa)	Poisson coefficient
2200	0.3

Table 2. Mechanical properties of the adhesive (Huntsman™ Araldite® 420 A/B epoxy resin)

In order to compute the initiation failure load, the initiation crack length and the displacement at initiation, a crack was initiated, on the one hand at the top right interface between the adhesive and the right substrate, and, on the other hand, at the bottom right interface. As the results obtained in these two configurations showed the initiation is more suitable to occur at the top right location of the interface, the following results concern the initiation of a debonding at this location.

The results obtained for three different adhesive thicknesses (0.1, 0.2 and 0.4 mm) regarding the evolutions of the initiation failure load, the initiation crack length and the displacement at initiation are respectively illustrated in Fig.2, Fig.3 and Fig.4.

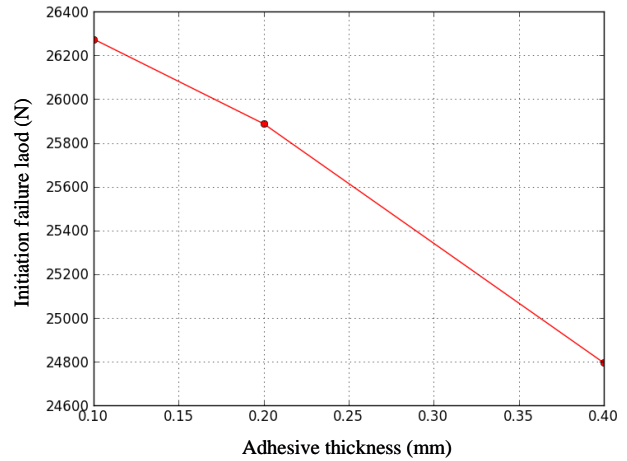


Fig. 2. Initiation failure load in function of the adhesive thickness

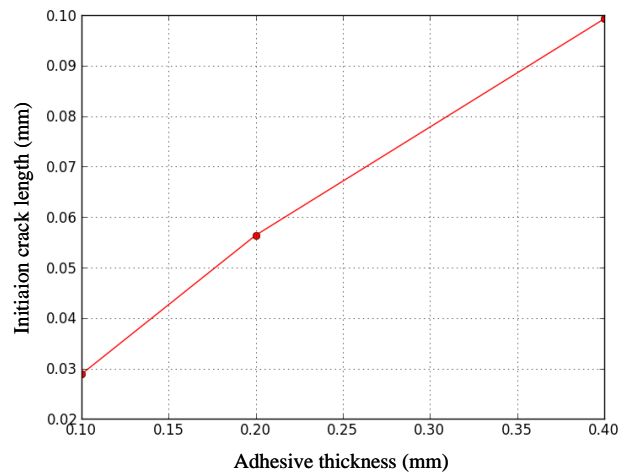


Fig. 3. Initiation crack length in function of the adhesive thickness

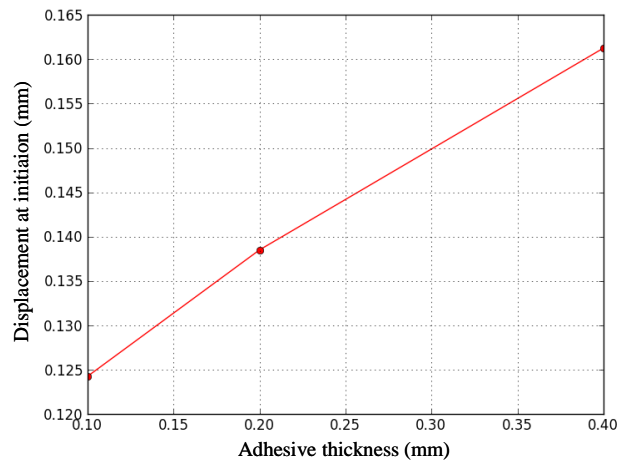


Fig. 4. Displacement at initiation in function of the adhesive thickness

First, these results show that the more the adhesive thickness increases, the more the initiation failure load of the bonded joint decreases. A thick adhesive has thus a bad influence on the initiation failure load of the bonded joint but a limited influence. Then, it is observed that the more the joint is thick, the more the initiation crack length is longer. The influence of the adhesive thickness on the initiation crack length is significative. But, as it is impossible to determine experimentally the initiation crack length, such assumption has to be taken with precaution. Finally, the displacement at initiation increases with the adhesive thickness highlighting a moderate influence of the adhesive thickness on the displacement at initiation.

As a conclusion, the adhesive thickness has an influence on the initiation. More precisely, it has a first order influence on the initiation crack length, a moderate influence on the displacement at initiation and a small influence on the initiation failure load. Therefore, in the following parts, this parameter is integrated into a CZM in order to evaluate the capabilities of this kind of model to describe the influence of the adhesive thickness on the debonding initiation.

3 Towards the proposal of a cohesive zone model suitable for the study of bonded joints

As a general approach here the objective is to propose one way to introduce the influence of the adhesive thickness on the initiation and to compare the results obtained with a CZM to the previous results.

Our choice to use a cohesive zone model implies the modeling of the adhesive thickness by an interface. So, the equivalent geometry to the one in Fig.1 is illustrated in Fig.5.

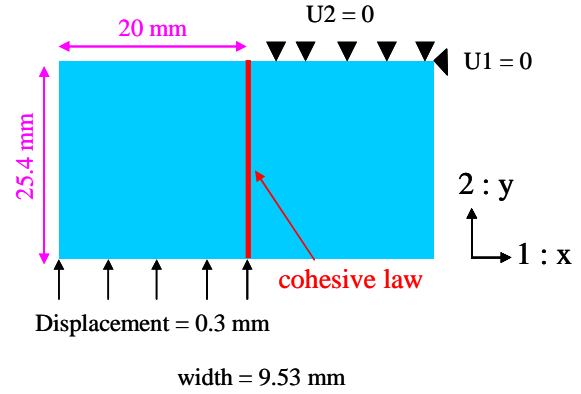


Fig. 5. Geometry, boundary conditions and load applied in the cohesive zone computations on the modified TAST

In a first part, a reminder of the general framework of a cohesive zone model formulation is given. Then, a study about the mesh size is realized in order to understand its influence on the description of the initiation. Then, the integration of the adhesive thickness in the softening law and its influence on the behavior of the bonded assembly are detailed. Finally, a study about the shape of the cohesive law is realized.

3.1 General framework of a cohesive zone model formulation

According to the framework proposed by Camanho [6], a cohesive zone model can be formulated as below :

$$\begin{aligned} \text{If } [u_n] \geq 0 & & \text{If } [u_n] < 0 \\ \begin{cases} T_n = K[u_n]f(\lambda) \\ T_{t,i} = K[u_{t,i}]f(\lambda) \end{cases} & & \begin{cases} T_n = \alpha_c K[u_n] \\ T_{t,i} = K[u_{t,i}]f(\lambda) \end{cases} \end{aligned} \quad (1)$$

with $i = 1,2$

where T_n (respectively $T_{t,1}$ and $T_{t,2}$) is the traction force in mode I (resp. in mode II and in mode III), $[u_n]$ (resp. $[u_{t,1}]$ and $[u_{t,2}]$) is the relative displacement upon mode I (resp. upon mode II and upon mode III), K is the initial stiffness of the interface (identical whatever the mode mixity (i.e. a combination of the fracture modes)) and α_c a

penalization parameter. $f(\lambda)$ is the function representing the damage effect and λ is the damage variable linked to the damage kinetic varying from 0 (unbroken state) to 1 (broken state). The interface law can take different shapes. Most of them have in common the interlaminar stress σ_c and the fracture toughness G_c . In our study, we chose to use a bi-linear law, a trapezoidal law and a tri-linear law. All of these laws propose an interfacial stiffness K .

3.2 Influence of the mesh size

The study about the mesh size convergence has been realized for mesh sizes of a mean value of 1 μm , 4 μm , 8 μm , 132 μm and 1 mm all along the overlap length between the substrates. The computation time with a mesh size of 1 μm exceeds the computation time with a mesh size of 1 mm of about 4.3 %.

The results obtained with the trapezoidal, bi-linear and tri-linear laws for an initial stiffness fixed at $K = 22000 \text{ N}\cdot\text{mm}^{-3}$ are respectively represented on Fig.6, Fig.7 and Fig.8.

On the one hand, with the trapezoidal law, there exists a good convergence between the results obtained with average mesh sizes of 1 μm , 4 μm and 8 μm , which is in agreement with the recommendation to have a refined mesh with CZM [7]. Similarly, with the bi-linear and tri-linear laws, the same result is observed even if, for a mesh size of 8 μm , there is a solution jump. On the other hand, the results obtained with mesh sizes of 132 μm and 1 mm do not describe sufficiently well the initiation and with these mesh sizes, we can observe many solution jumps. So, the more appropriate mesh size to have the lowest computation costs is a mesh size of 8 μm .

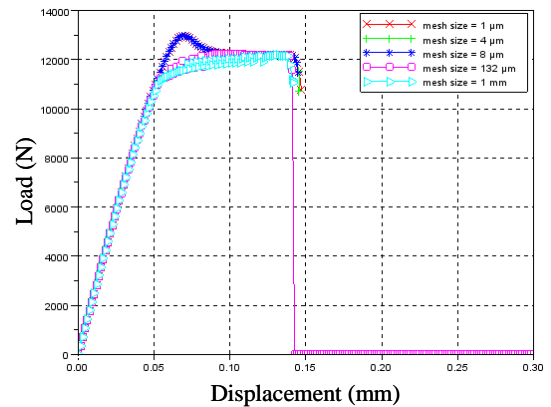


Fig. 6. Influence of the cohesive mesh size on the load/displacement curve with the trapezoidal law

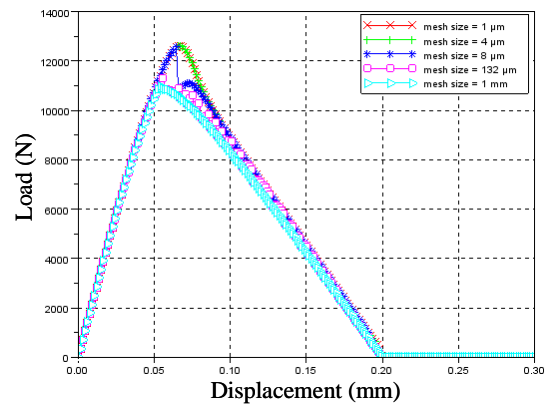


Fig. 7. Influence of the cohesive mesh size on the load/displacement curve with the bi-linear law

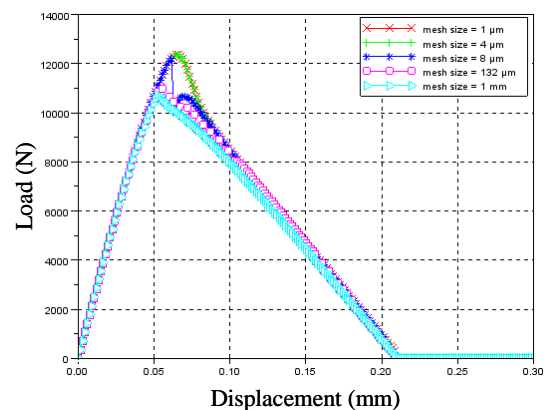


Fig. 8. Influence of the cohesive mesh size on the load/displacement curve with the tri-linear law

Having analyzed the influence of the mesh size on the behavior, we can study the influence of the shape of the interface law on the behavior and the initiation too.

3.3 Influence of the shape of the interface law

If for a stable and rectilinear propagation the influence of the shape of the interface law is negligible [8], it is still an open question for initiation. In order to answer to this question, the analysis of the evolution of the load in function of the applied displacement has been realized for three different values of stiffness with the same three interface laws than previously. The computations run with the trapezoidal law for an initial stiffness fixed at $K = 22000 \text{ N.mm}^{-3}$ and fixed at $K = 11000 \text{ N.mm}^{-3}$ did not guarantee the convergence while the computation with $K = 5500 \text{ N.mm}^{-3}$ did. So the macroscopic responses obtained with the three laws for $K = 5500 \text{ N.mm}^{-3}$ are illustrated in Fig. 9.

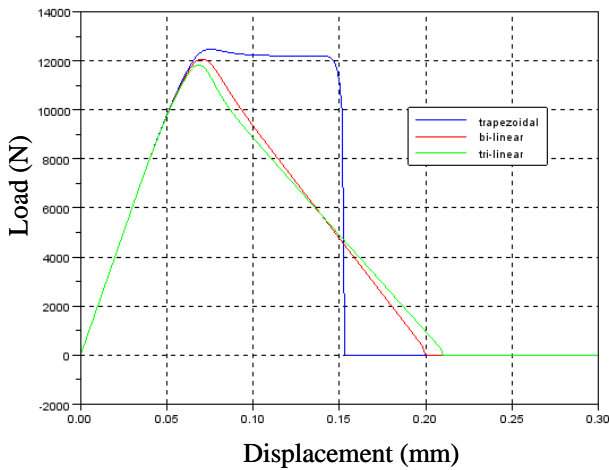


Fig. 9. Influence of the shape of the interface law on the load/displacement curve

Firstly, we aimed to understand the difference of behaviors obtained between the three laws. For that, we studied the evolution of the damage variable λ on each Gauss point all along the interface for the three laws for different displacements. The evolution of the process zone was observed at four particular displacements which have been located on the load/displacement curve in Fig. 10.

At d_{\max} , almost simultaneously, the load attains a maximum value for the three laws. The other displacements considered correspond to the displacements at failure for the three laws, *i.e.* the displacement at failure for the trapezoidal law

d_{trapez} , for the bi-linear law d_{bi} and for the tri-linear law d_{tri} .

The process zone evolutions are illustrated for the three laws at the displacement d_{\max} (Fig.11) and at the displacements at failure d_{trapez} (Fig.12), d_{bi} (Fig.13), d_{tri} (Fig.14).

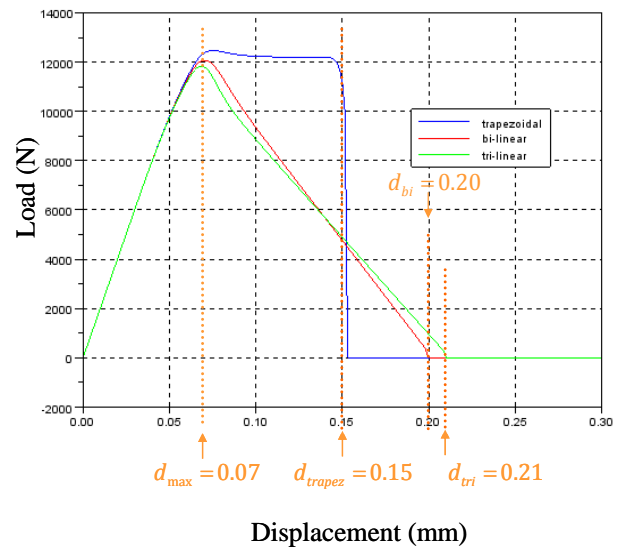


Fig. 10. Location of the displacements considered on the load/displacement curve

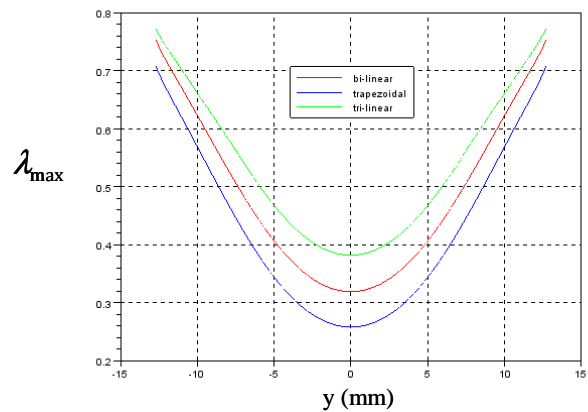


Fig. 11. Evolution of the process zone at $d_{\max} = 0.07$

Before failure, at d_{\max} , the process zone of the trapezoidal law is less damaged than the ones of the

bi-linear and tri-linear laws. This observation could explain that the interface supports better the load with the trapezoidal law than with the other laws. That is why, at d_{\max} , the load is higher with the trapezoidal law than with the other ones.

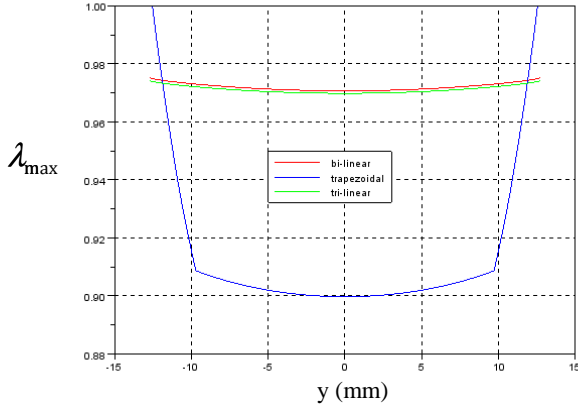


Fig. 12. Evolution of the process zone at $d_{\text{trapez}} = 0.15$

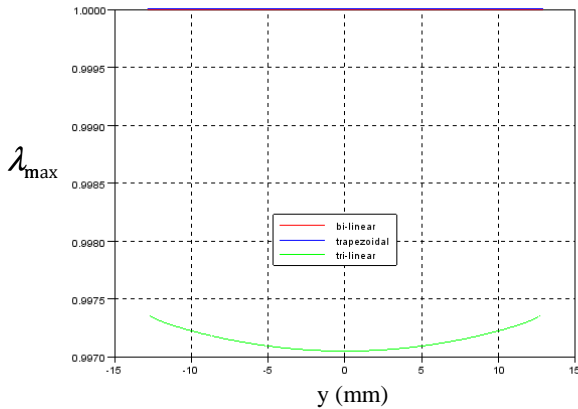


Fig. 13. Evolution of the process zone at $d_{\text{bi}} = 0.20$

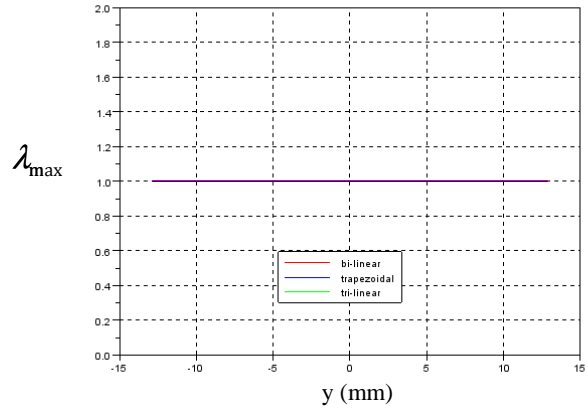


Fig. 14. Evolution of the process zone at $d_{\text{tri}} = 0.21$

In order to enrich our understanding of the difference observed in behaviors, we wanted to know whether it may exist a kind of continuity in the behaviors obtained between the three laws. According to us, the bi-linear law present a shape that we can assimilate to the shape of a trapezoidal law for which the length of the plateau (controlled by the parameter α_δ in the trapezoidal cohesive law) would be null (*i.e.* with $\alpha_\delta = 0$) (Fig.15). So in order to understand why with the trapezoidal law the behavior is so far from the behaviors with the two other laws, we performed more computations with the trapezoidal law but with a modification of the length of the plateau when the traction force attains σ_c as illustrated in Fig.16. The two additional computations were performed with the trapezoidal law with $\alpha_\delta = 0.5$ and $\alpha_\delta = 0.2$ instead of the default value $\alpha_\delta = 0.9$ in the previous simulation with the trapezoidal law. The macroscopic responses obtained with the trapezoidal law with $\alpha_\delta = 0.5$ and $\alpha_\delta = 0.2$ are compared to the previous macroscopic responses obtained with the bi-linear and tri-linear laws and with the trapezoidal law with $\alpha_\delta = 0.9$ in Fig.17.

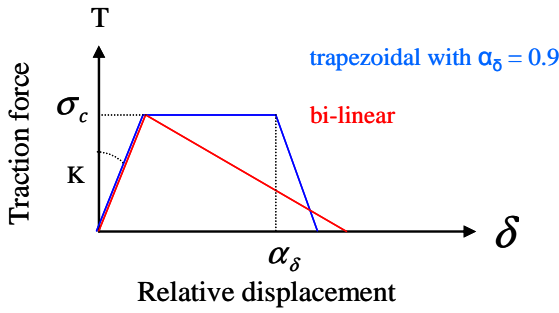


Fig. 15. Representation of the bi-linear and trapezoidal laws

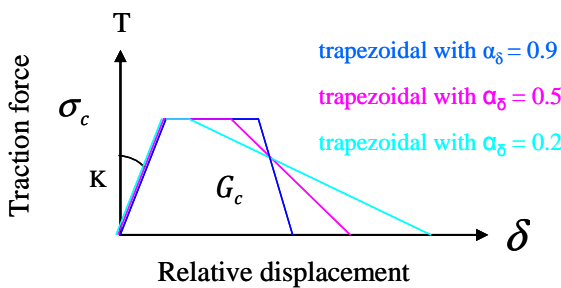


Fig. 16. Three trapezoidal laws used with different lengths of plateau when the cohesive force is σ_c

As we can see in Fig.17, the length of the plateau strongly influences the macroscopic answer. This parameter has to be included in a CZM to study the initiation of the debonding in a bonded assembly. Moreover, when the length of the plateau with a trapezoidal law decreases, the behavior becomes closer to the behavior obtained with a bi-linear law. Therefore, there exists a kind of continuity of the behavior between the three laws although it does not seem obvious at first sight.

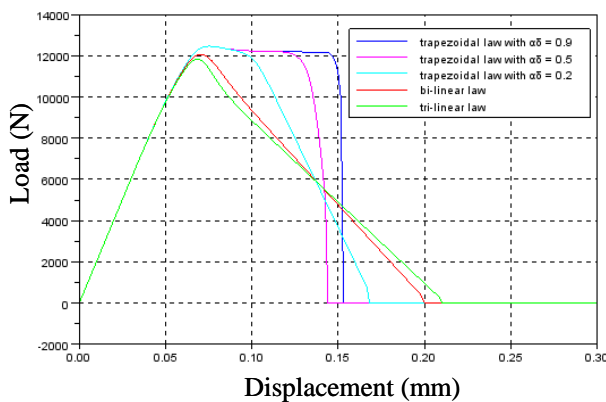


Fig. 17. Relation between the different shapes of the interface laws on the behavior

Secondly, we aimed to understand why the displacement at failure is different from one law to another. For that, we looked at the previous evolutions of the process zone (Fig.11 to Fig.14). We noticed therefore that the entire interface is damaged and that the failure occurs always when $\lambda = 1$ for the same Gauss points (the points at both extremities of the interface) for the three laws. Therefore, it seems us that the differences regarding the displacements at failure with the different laws can be explained by the existence of different values of the relative displacement when the interface is

broken (δ_f) for each law. Indeed, as illustrated in Fig. 18, with the same cohesive parameters (*i.e.* the toughness G_c and the interfacial strength σ_c), we can notice that locally, for both Gauss points at the extremities of the geometry which have been considered, $\delta_{f\text{trapezoidal}} < \delta_{f\text{bilinear}} < \delta_{f\text{trilinear}}$. That is why the displacement at failure is different from one law to another and that in an ascending order, the displacement at failure is attained first with the trapezoidal law, then with the bi-linear law and finally with the tri-linear law.

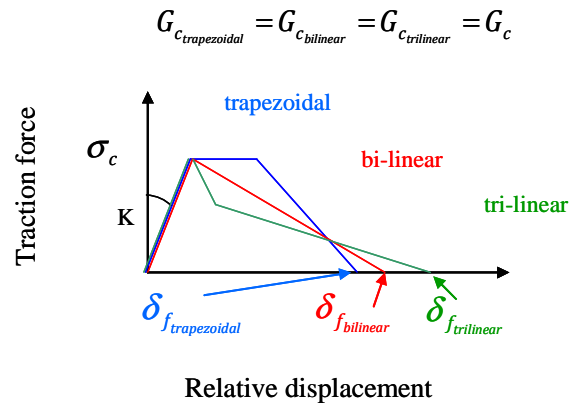


Fig. 18. Representation of the critical relative displacements when the interface is broken for the three cohesive laws for a given (σ_c, G_c) couple

Thirdly, we aimed to understand the influence of the law shape on the initiation failure load. But we observe that the initiation failure load, defined to be the load for which $\lambda = 1$ for the first time, is null whatever the law. So the initiation failure load may rather correspond to the maximum load the interface can bear before failure. To verify this hypothesis it is

necessary to determine the energy dissipated locally by each law at the moment where the maximum load is reached. If the maximum energy has been spent at that state, the maximum load could be considered as the initiation failure load and consequently the trend observed with elastic computations could be verified here. But if the energy spent is insufficient, the trend observed with elastic computations could not be verified here. However, the modified TAST having a mode mixity which is evolving during the load, it is not an easy task to determine this energy. Thus, it is not possible to conclude about the fact that the initiation failure load corresponds to the maximum load. Nevertheless, the maximum load is different from one law to another and it can be explained. Indeed, the maximum loads are about:

- 12470 N for the trapezoidal law
- 12000 N for the bi-linear law
- 11833 N for the tri-linear law

So the initiation failure load is the highest with the trapezoidal law. The process zone being less damaged for the trapezoidal law than for the other laws and the displacement at failure being the lowest, it can explain a high initiation failure load with the trapezoidal law. The failure load with the bi-linear law is lower than with the trapezoidal law but higher than with the tri-linear law because the evolution of the damage in the process zone and the displacement at failure are intermediate compared to the results with the other laws. Finally, because of the most damaged interface and the highest displacement at initiation, the tri-linear law is the one having the lowest maximum load.

To conclude, it is now obvious that the shape of the law in the cohesive zone model seems to play at major order on the modeling of the initiation of a debonding. In fact, the behavior, the displacement at failure and the maximum load depend on the shape of the model used.

Firstly, the behavior is totally different from one law to another. In fact, the length of the plateau in the trapezoidal law strongly influences the macroscopic answer and that is why this parameter has to be included in a CZM to study the initiation of the debonding in a bonded assembly. Moreover, there exists a continuity of the behavior between the three different laws, the bi-linear law being considered as a trapezoidal law without plateau (with $\alpha_\delta = 0$).

Secondly, in an ascending order, the displacement at failure is attained first with the trapezoidal law, then with the bi-linear law and finally with the tri-linear law. The reason explaining this observation relies on the results about the critical relative displacement when the interface is broken.

Finally, the maximum load is different from one law to another because of the damage state in the process zone and the displacement at failure for each law.

3.4 Influence of the stiffness on the initiation

From the CZM formulation (1), it is possible to make appear the adhesive thickness (here in mode I) :

$$T_n = K[u_n] = Ke \frac{[u_n]}{e} \quad (2)$$

Besides, with the Hooke's law, we can link the traction force in mode I T_n to the deformation ε through the Young's modulus E :

$$T_n = E\varepsilon = E \frac{[u_n]}{e} \quad (3)$$

So, by combining (2) and (3) :

$$K = \frac{E}{e} \quad (4)$$

with E the Young modulus of the adhesive and e its thickness. Therefore, for a given adhesive, by varying K , theoretically, we make vary the adhesive thickness.

In order to highlight the influence of the stiffness K on the initiation failure load, computations with several values of the initial stiffness of the CZM have been realized on the modified TAST presented above (Fig.5)

The mechanical properties of the substrates remain the same than previously (Table 1). The interface properties are summarized in Table 3.

Strength in mode I (MPa)	Strength in mode II (MPa)	Toughness in mode I (J/m ²)	Toughness in mode II (J/m ²)
35	50	2800	5000

Table 3. Interface properties

The influence of the initial stiffness K on the initiation has been studied for three values. Each stiffness is representative of a physical adhesive thickness, the Young modulus E of the adhesive being supposed equal to 2200 MPa (Table 2). The Table 4 put face to face the values of the stiffnesses studied and their corresponding physical adhesive thicknesses aimed to be studied.

Stiffness ($\text{N}\cdot\text{mm}^{-3}$)	Adhesive thickness (mm)
22000	0.1
11000	0.2
5500	0.4

Table 4. Corresponding physical adhesive thicknesses to the cohesive stiffnesses

The macroscopic responses obtained by varying the stiffness K are illustrated respectively with the trapezoidal law, the bi-linear law and the tri-linear law in Fig. 19, Fig. 20 and Fig. 21.

Whatever the law used, there exists an influence of the cohesive stiffness on the behavior because the macroscopic stiffness increases as the cohesive stiffness increases while the load increases until attaining a maximum load. Nevertheless, the influence of the cohesive stiffness on the initiation failure load is not verified as evidenced in 3.3 but is on the maximum load. So, the trend observed with elastic computations and the use of the coupled criterion is not easy to integrate in cohesive zone models only by varying the cohesive stiffness.

Moreover, it can be noticed that the macroscopic response obtained with each law is very similar to the cohesive law shape. This observation can be explained by the fact that the entire interface is damaged, thus the process zone is much extended. Nevertheless, as the macroscopic response is not absolutely identical to the local law shape, there exists a contribution of the substrates behavior on the macroscopic response. Besides, the damage being different all along the interface during the loading, it can explain that the macroscopic response is not totally identical to the cohesive law shape (evidenced in Fig. 11 to Fig. 14).

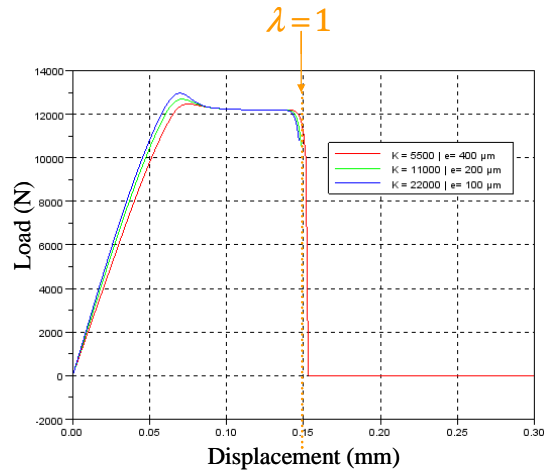


Fig. 19. Influence of the cohesive stiffness K on the load/displacement curve with the trapezoidal law

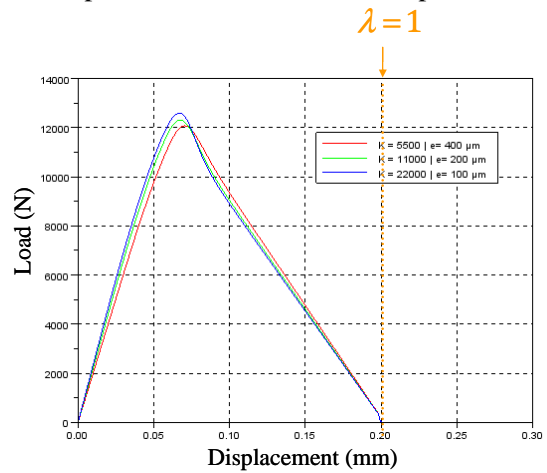


Fig. 20. Influence of the cohesive stiffness K on the load/displacement curve with the bi-linear law

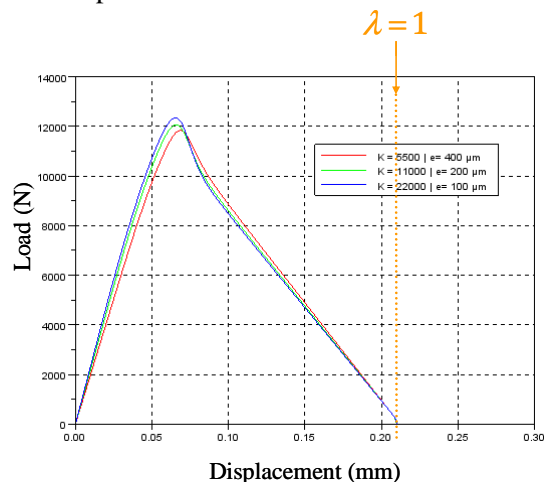


Fig. 21. Influence of the cohesive stiffness K on the load/displacement curve with the tri-linear law

Having analyzed the influence of the stiffness on the behavior with different interface laws, a comparison between the results obtained with elastic computations by using the coupled criterion and the results obtained with the CZM is realized.

4 Comparison between the results obtained with elastic computations by using the coupled criterion and the results obtained with the CZM

As we obtained results with two approaches based on the same criteria to predict the initiation, the aim is here to compare them to conclude on the relevance and the accuracy of the CZM proposed to be suitable to the study of bonded joints by taking into account the influence of the adhesive thickness on the initiation.

In order to simulate the same test than the one illustrated in Fig.1, it has been necessary in the CZM to impose stronger cohesive properties to imply an initiation at the top right of the interface.

As the modified TAST is a test in mode II, the cohesive stiffness corresponds rather to :

$$K = \frac{G}{e} \quad (5)$$

with e the adhesive thickness and G the shear modulus of the adhesive given by :

$$G = \frac{E}{2(1+\nu)} \quad (6)$$

where ν is the Poisson coefficient of the adhesive and $E = 2200$ MPa is the longitudinal Young's modulus of the adhesive.

Using a CZM with no thickness is not the same than using a volumic model with a high number of elements in the adhesive thickness. So a readjustment of the stiffness of the macroscopic response obtained with cohesive zone computations (CZC) on the one obtained with elastic computations (EC) has been realized. In that purpose the readjusted initial cohesive stiffness $G = 836$ MPa was used. The results obtained with the two approaches are compared for three adhesive

thicknesses 0.1 mm, 0.2 mm and 0.4 mm respectively in Fig.22, Fig.23 and Fig.24.

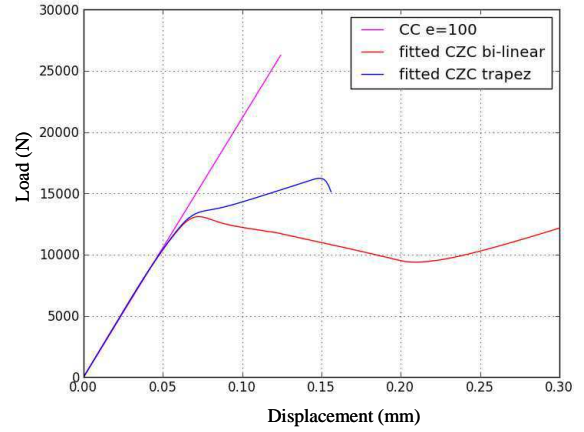


Fig. 22. Comparison for $e = 0,1$ mm / $K = 8360$ $N.mm^{-3}$

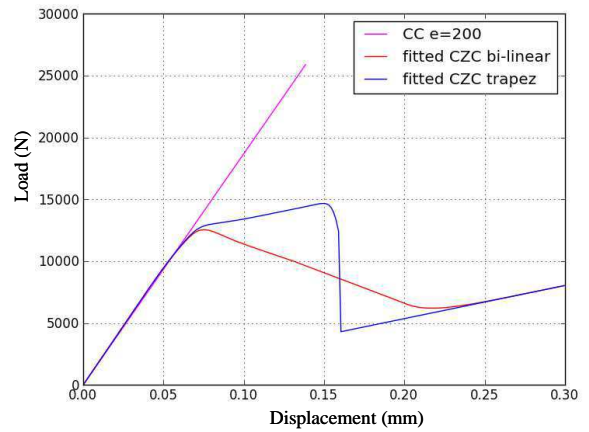


Fig. 23. Comparison for $e = 0,2$ mm / $K = 4180$ $N.mm^{-3}$

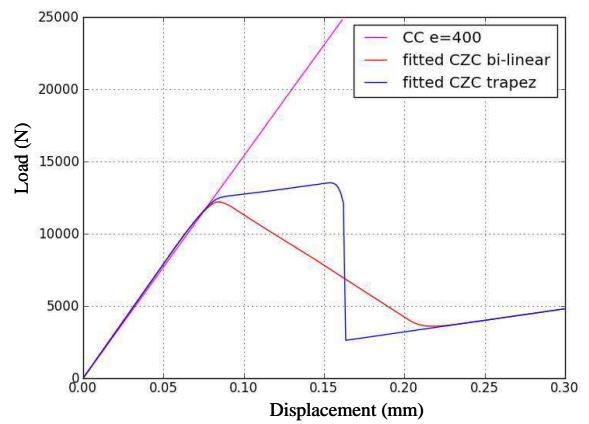


Fig. 24. Comparison for $e = 0,4$ mm / $K = 2090$ $N.mm^{-3}$

The two approaches present a different displacement at initiation. Maybe, in the cohesive model, the major part of its energy has been dissipated at the displacement at initiation determined with the EC and the CC. To verify this hypothesis, it is necessary to compute the energy spent locally with both bi-linear and trapezoidal laws. It is easy to compute it here because by having imposed stronger cohesive properties on one side, this test becomes a pure-mode II test. So the computation of the energy for each law informs us that, with the trapezoidal law, all the energy has been spent (5000 J/m²) when the displacement at initiation is attained with the EC. Besides, with the trapezoidal law, as more energy was spent before attaining its displacement at initiation, a solution jump occurred. But, with the bi-linear law, 92 % have been spent at the same state. For the tri-linear law, as the stronger interface failed since the beginning, this law won't be compared to the elastic approach. So it seems that the displacement at initiation for the trapezoidal law is sufficiently close to the one obtained with EC and the CC.

Moreover, the two approaches present different initiation failure loads for each adhesive thickness. Indeed, the initiation failure loads are higher with the EC than the ones obtained with CZM for both cohesive laws.

Finally, the stiffness of the macroscopic response obtained with the CZC seem to be in a good agreement with the stiffness of the one obtained with the volumic model for a given adhesive thickness / cohesive stiffness couple.

5 Conclusions and perspectives

In order to predict the initiation of a debonding in a 3D structure and in presence of non-linear behaviors, the choice to use a cohesive zone model imposed itself. In order to adapt a cohesive model to the study of initiation in a bonded joint, the integration of the adhesive properties influence seemed necessary. Among the properties of an adhesive, its thickness is a parameter that plays a role at major order on the initiation. That is why we looked forward to integrate its influence in the cohesive zone model.

For that, it was first necessary to highlight the influence of the adhesive thickness on the initiation failure load. This was realized with the coupled criterion composed of the same ingredients than the CZM. Finally, this study demonstrated that varying the adhesive thickness has a greater effect on the displacement at initiation than on the initiation failure load.

Then, with CZM, a mesh size convergence highlighted the importance of a very refined mesh to catch the initiation. We will in particular underline here the necessity to use mesh sizes of the micrometer order for the initiation description while mesh sizes of the millimeter order were enough satisfying for the propagation description.

Besides, we saw that the law shape had a major order influence on the behavior of the interface but on the initiation failure load and on the displacement at failure too. Therefore, it seems necessary to define which law is the more relevant to describe the initiation of a debonding in a bonded assembly. For that, initiation tests controlled by the stress criterion and not by the energy one are currently under realization in order to make an inverse identification. Moreover, these tests will enable to validate the model.

Finally, we integrated the influence of the adhesive thickness through the use of the cohesive stiffness. Thus, the influence of the cohesive stiffness on the behavior has been shown. But, the initiation failure load remains the same whatever the cohesive stiffness. However, the displacement at initiation obtained with the trapezoidal law is close to the one obtained with EC. By comparing the volumic model and the CZM, a readjustment has been proposed to make the stiffness of the macroscopic responses match together. This modification seems satisfying to describe the influence of the adhesive thickness on the stiffness. Further work has to be done to obtain a good agreement between the two approaches on the initiation failure load and on the displacement at initiation, maybe by integrating more adhesive properties.

Acknowledgments

This work was supported under the PRC Composites, French research project funded by DGAC, involving SAFRAN Group, ONERA and CNRS.

References

- [1] L. Lagunegrand, T. Lorriot, R. Harry, H. Wargnier and J.M. Quenisset "Initiation of free-edge delamination in composite laminates." *Composites Science and Technology*, Vol. 66, pp 1315-1327, 2006.
- [2] D. Leguillon "Strength or toughness ? A criterion for crack onset at a notch." *European Journal of Mechanics A/Solids*, Vol. 21, pp 61-72, 2003.
- [3] Turon, A., Camanho, P.P. and Renart, J. "Accurate simulation of delamination growth under mixed-mode loading using cohesive elements : definition of intralaminar strengths and elastic stiffness." *Composite Structures*, Vol. 92, pp 1857-1864, 2010.
- [4] Vandellos, T., Huchette, C. and Carrère, N.. "Proposition of a framework for the developpement of a cohesive zone model adapted to Carbon-Fiber Reinforced Plastic laminated composites", *Composite Structures*, In Press, Accepted Manuscript, 2013.
- [5] Cognard, J.Y., Creac'hcadec, R. and Maurice, J. "Numerical analysis of the stress distribution in single-lap shear tests under elastic assumption – Application to the optimisation of the mechanical behavior", *International Journal of Adhesion and Adhesives*, Vol. 31, pp 715-724, 2011.
- [6] Camanho, P.P. and Davila, C.G. "Mixed-mode decohesion finite elements for simulation of delamination in composite materials", *NASA/TM-2002-211737*, 2002.
- [7] Turon, A., Davila, C.G., Camanho, P.P. and Costa, J. "An engineering solution for mesh size effects in the simulation of delamination using cohesive zone models", *Engineering Fracture Mechanics*, 2007.
- [8] Monerie, Y. and Acary, V. "Formulation dynamique d'un modèle de zone cohésive tridimensionnel couplant endommagement et frottement", *Revue Européenne des Eléments Finis*, Vol. 10, pp 489-503, 2001.